

DYNAMICAL BIAS IN THE COIN TOSS

Persi Diaconis

Departments of Mathematics
and Statistics
Stanford University

Susan Holmes

Department of Statistics
Sequoia Hall
Stanford University

Richard Montgomery

Department of Mathematics
University of California
Santa Cruz

Abstract

We analyze the natural process of flipping a coin which is caught in the hand. We prove that vigorously-flipped coins are biased to come up the same way they started. The amount of bias depends on a single parameter, the angle between the normal to the coin and the angular momentum vector. Measurements of this parameter based on high-speed photography are reported. For natural flips, the chance of coming up as started is about .51.

Introduction

Coin-tossing is a basic example of a random phenomenon. However, naturally tossed coins obey the laws of mechanics (we neglect air resistance) and their flight is determined by their initial conditions. Figure 1 a-d shows a coin-tossing machine. The coin is placed on a spring, the spring released by a ratchet, the coin flips up doing a natural spin and lands in the cup. With careful adjustment, the coin started heads up always lands heads up – one hundred percent of the time. We conclude that coin-tossing is ‘physics’ not ‘random’.

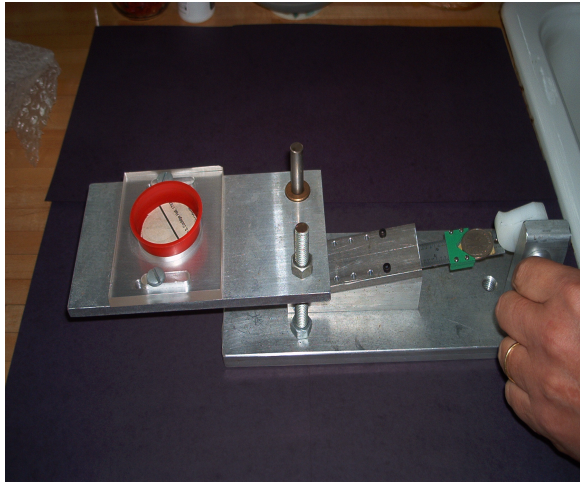


Figure 1.a

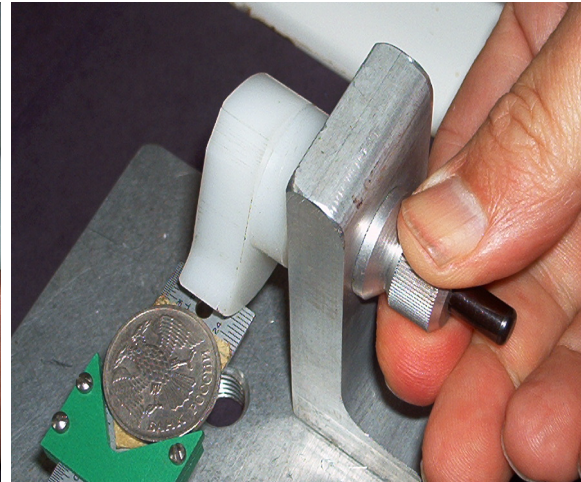


Figure 1.b



Figure 1.c

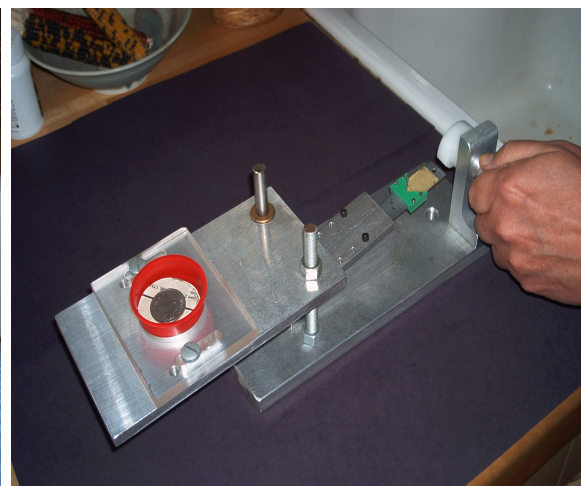


Figure 1.d

Joe Keller [Keller, 1986] carried out a study of the physics assuming that the coin spins about an axis through its plane. Then, the initial upward velocity and the rate of spin determine the final outcome. Keller showed that in the limit of large initial velocity and large rate of spin, a vigorous flip, caught in the hand without bouncing, lands heads half the time. This work is described more carefully in Section Two which contains a literature review of previous work on tossed and spinning coins.

The present paper takes precession into account. Real flips often precess a fair amount and this changes the conclusion. Consider first a coin starting heads up and hit exactly in the center so it goes up without turning like a pizza. We call such a flip a “total cheat coin”, because it always comes up the way it started. For such a toss, the angular momentum vector \vec{M} lies along the normal to the coin.

In Section Three we prove that the angle ψ between \vec{M} and the normal to the coin stays constant. If this angle is less than 45° , the coin never turns over. It wobbles around and always comes up the way it started. Magicians and gamblers can carry out such controlled flips which appear visually indistinguishable from normal flips. For Keller’s analysis, \vec{M} is assumed to lie in the plane of the coin making angle 90° with the normal to the coin.

We state our main theorems first.

Theorem 1 *For a coin tossed starting heads up at time 0 the cosine of the angle between the normal to the coin at time t and the up direction is*

$$(1) \quad f(t) = A + B \cos(\omega_N t)$$

with $A = \cos^2 \psi$, $B = \sin^2 \psi$, $\omega_N = \|\vec{M}\|/I_1$, $I_1 = \frac{1}{4}mR^2 + \frac{1}{3}mh^2$ for coins with radius R , thickness h and mass m . Here ψ is the angle between the angular momentum vector \vec{M} and the normal at time $t = 0$.

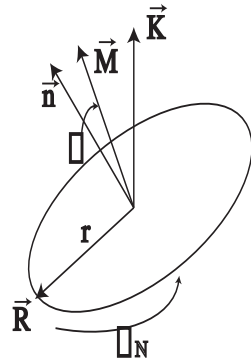


Figure 2: Coordinates of Precessing Coin.

To apply theorem 1, consider any smooth probability density g on the initial conditions (ω_N, t) of Theorem 1. Keep ψ as a free parameter. We suppose g to be centered at (ω_0, t_0) so that the resulting density can be written in the form $g(\omega_N - \omega_0, t - t_0)$. Let (ω_0, t_0) tend to infinity along a ray in the positive orthant $\omega_N > 0, t > 0$, corresponding to large spin, and large time-of-flight.

Theorem 2 . For all smooth, compactly supported densities g , the limiting probability of heads $p(\psi)$ with ψ fixed, given that heads starts up, is given by

$$(2). \quad p(\psi) = \begin{cases} \frac{1}{2} + \frac{1}{\pi} \sin^{-1}(\cot^2(\psi)) & \text{if } \frac{\pi}{4} < \psi < 3\pi/4 \\ 1 & \text{if } 0 < \psi < \pi/4 \text{ or } \frac{3\pi}{4} < \psi < \pi. \end{cases}$$

A graph of $p(\psi)$ appears in Figure 3. Observe that $p(\psi)$ is always greater than or equal to $1/2$ and equals $1/2$ only if $\psi = \pi/2$. In this sense, vigorously tossed coins $((w_0, t_0)$ large) are biased to come up as they started, for essentially *arbitrary* initial distributions g . The proof of Theorem 2 gives a quantitative rate of convergence to $p(\psi)$ as w_0 and t_0 become large.

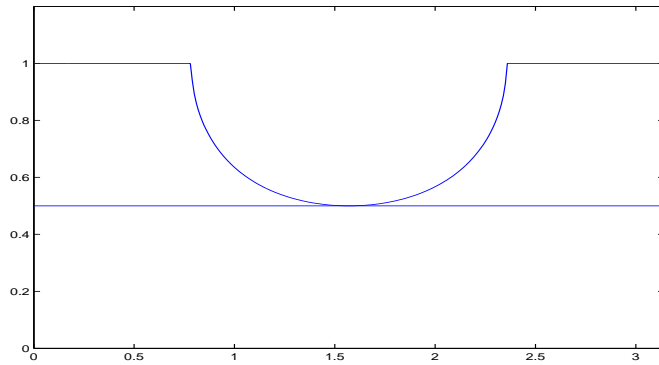


Figure 3: $p(\psi)$

We now explain the picture behind Theorem 1 and some heuristics for Theorem 2. The angular momentum vector is constant in time and the normal vector precesses around it at a uniform velocity, sweeping out a circle on the sphere of unit vectors. (This is proved in section 3.) On this sphere, draw the equator of vectors orthogonal to the direction \vec{K} of “straight up”. Points on the equator represent the coin edge-on. Points in the upper hemisphere H represent the coin ‘heads up’ and points in the lower hemisphere T represent the coin ‘tails up’. H corresponds to $f > 0$ and T to $f < 0$ where f is the function of theorem 1.

Suppose now that the coin starts its travel precisely heads up – so that the normal is aligned with \vec{K} . Then the normal \vec{N} traces out a circle on the sphere passing through \vec{K} and having center the “random” point \vec{M} (normalized). For all choices of \vec{M} **except** for \vec{M} lying in the equator (the Keller flip) more of this circle lies in the H hemisphere than the T. The coin appears biased towards heads.

To obtain a quantitative expression for the bias we fix the angle ψ , which is also the (spherical) radius of the circle described by the normal. To begin, note that if ψ is between 0 and $\pi/4$ then $A > B$ and $f(t) > 0$ for all time t . In this case the coin is always heads up and

we are in the range where $p = 1$ in theorem 2. In general, it is plausible that the probability of heads is proportional to the amount of time which \vec{N} spends in the hemisphere H. This proportion of time is precisely the $p(\psi)$ in theorem 2 above.

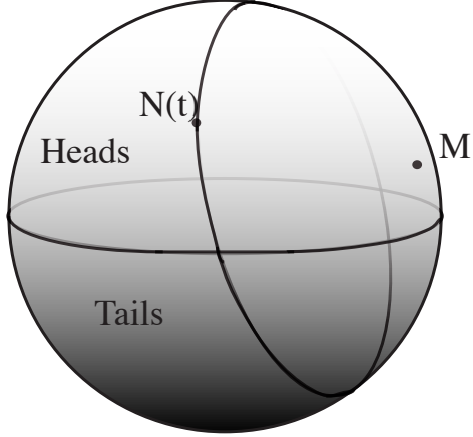


Figure 4: The normals to the coin lie on a circle intersecting with the equator of change of sides.

Figures 5a and 5b show the effect of changing ψ . In Figure 5a, $\psi = \frac{\pi}{2}$ and f is positive half of the time. In Figure 5b, $\psi = \frac{\pi}{3}$ and f is more often positive.

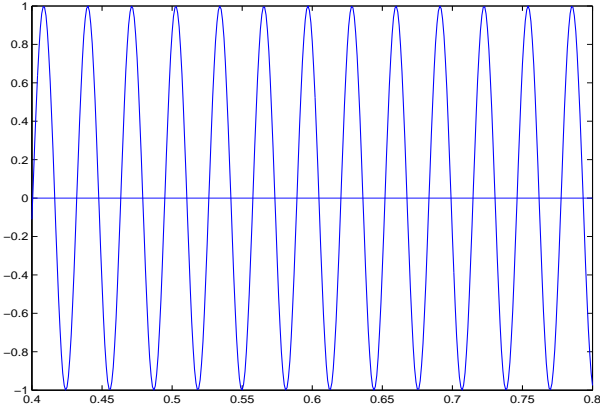


Figure 5a: $\psi = \pi/2$

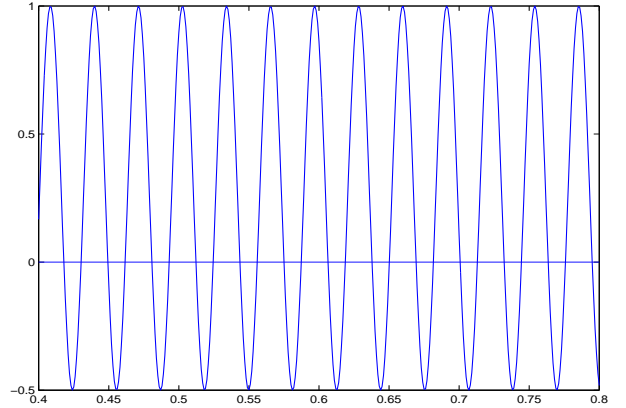


Figure 5b: $\psi = \pi/3$

Theorems 1 and 2 lead us to ask what is the empirical distribution of ψ when real people toss coins. In Section 5 two empirical studies are described. The first is low-tech and uses a coin with a thin ribbon attached. The second uses a high-speed slow motion camera. The projection of a circle onto the plane of the camera is an ellipse. Using image analysis techniques we fit the ellipses to the images of the tossed coin. A simple function of the lengths of the major and minor axes gives the normal to the coin in three-space. As

explained, these normals spin in a circle about the angular momentum vector which stays fixed during the coin's flight. This gives an estimate of ψ . Two methods of estimation which agree to reasonable approximation are given.

The empirical estimates of ψ show that naturally flipped coins precess sufficiently to force a bias of at least .01. We find it surprising that this bias persists in the limit of vigorously flipped coins for general densities $g(\omega_N, t)$.

The structure of the rest of the paper is as follows. Section 2 reviews previous literature and data on coin-tossing. Section 3 reviews rigid body motion and proves Theorem 1. In section 3 we also derive an exact result for the amount of precession: the amount that the coin turns about its normal during one revolution of the normal about the angular momentum vector is $\pi \cos(\psi)$. This is an example of a Berry phase. The limiting results of Theorem 2 are proved in Section 4. Section 5 presents our data. Section 6 presents some caveats to the analysis along with our conclusions.

2. Previous Literature

The analysis of classical randomization devices using mechanics and a distribution on initial conditions goes back to Poincaré's analysis of roulette [Poincaré,1896],page 122-130. This was brilliantly continued in a sequence of studies by Hopf [Hopf,1934, Hopf,1936, Hopf,1937] who studied Buffon's needle, introduced various mixing conditions to *prove* independence of successive outcomes and gave examples where the initial conditions do not wash out. Hopf began a classification of low order ordinary differential equations by sensitivity to initial conditions. While this work is little known today, [von Plato,1994] gives some further history, [Strevens, 2003] offers a philosopher's commentary and [Engel, 1992] presents a detailed development with extensions.

It cannot be emphasized too strongly that the results above are limiting results: Poincaré's arguments suggest that as a roulette ball is spun more and more vigorously the numbers become closer and closer to uniformly distributed. There are numerous studies ([Barnhart, 1992], [Bass, 1985]) suggesting that real roulette may not be vigorous enough to wash out the initial conditions.

The careful study of flipped coins was begun by [Keller, 1986], whose analysis we briefly sketch here. He assumed that a coin flips about an axis in its plane with spin about this axis at rate ω revolutions per second. If the initial velocity in the up direction \vec{K} is v_z , after t seconds, a coin flipped from initial height z_0 will be at height $z_0 + tv_z - (g/2)t^2$. Here g is the acceleration due to gravity ($g = 32 \text{ ft}/(\text{sec})^2$ if height is measured in feet). If the coin is caught when it returns to z_0 , the elapsed time t^* satisfies $z_0 + t^*v_z - (g/2)(t^*)^2 = z_0$ or $t^* = v_z/(g/2)$. The coin will have revolved $\omega v_z/(g/2)$ times. If this is between $2j$ and $2j + 1$ the initial side will be up-most. If it is between $2j + 1$ and $2j + 2$ the opposite side

will be up-most. Figure 6 shows the decomposition of the phase space (ω, t) into regions where the coin comes up as it started or opposite. The edges of the regions are along the hyperbolae $\omega v / (g/2) = j$. Visually, the regions get close together so small changes in the initial conditions make for the difference between heads and tails.

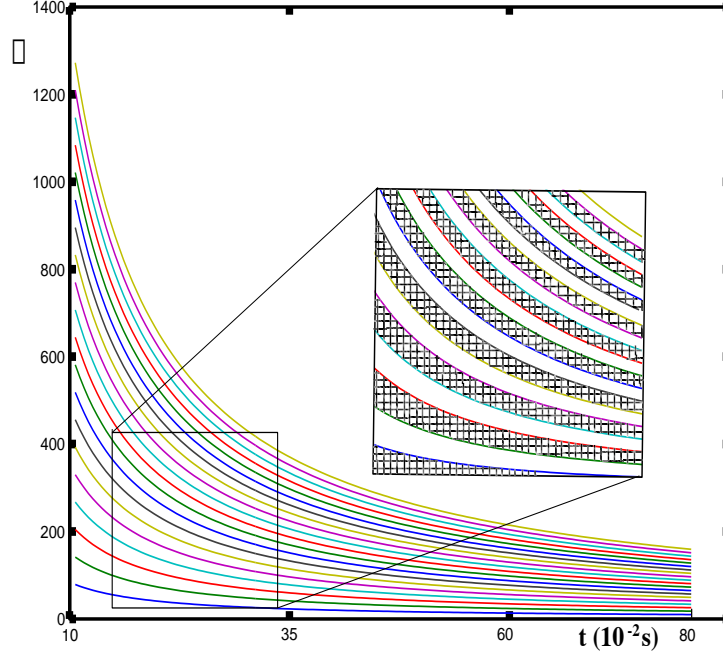


Figure 6: Hyperbolae as defined by the various initial values of ω .

The spaces between the hyperbolae in Figure 6 have equal area.

The horizontal axis goes from $t = 0.1$ to $t = 0.8$.

[Engel, 1992] offers a way to get around asymptotic limits by deriving explicit error terms for the approximations. Here is one of his theorems, specialized to the coin-tossing case. Let $f(\omega, v)$ be a probability density on the $\omega - v$ plane. Thus $f(\omega, v) \geq 0$ and $\int \int f(\omega, v)d\omega dv = 1$. The marginal densities $f_1(\omega), f_2(v)$ are defined by

$$f_1(\omega) = \int f(\omega, v)dv \quad f_2(v) = \int f(\omega, v)d\omega.$$

The conditional densities $f_\omega(v)$ and $f_v(\omega)$ are defined by

$$f_\omega(v) = \frac{f(\omega, v)}{f_1(\omega)}, \quad f_v(\omega) = \frac{f(\omega, v)}{f_2(v)}.$$

Thus $f_\omega(v)$ is the probability density which gives the chance that a random quantity with density $f(\omega, v)$ is in $(v, v + dv)$ given an observed, fixed value of ω . The following theorem applies to the case where $\psi = \pi/2$.

Theorem (Engel-Kemperman). Let $f(\omega, v)$ be a probability density on the (ω, v) plane with marginal densities $f(\omega), f(v)$, differentiable conditional densities $f_\omega(v), f_v(\omega)$. Translate f to $f(v + v_0, \omega + v_0)$. Then, the probability over the heads region in Figure 6 (the Keller coin) satisfies

$$\left| P(\text{heads}) - \frac{1}{2} \right| \leq 4\pi \min \left(\frac{V_v}{v_0}, \frac{V_\omega}{\omega_0} \right)$$

where

$$V_v = \int \int |f'_v(\omega)| f(\omega) d\omega dv, \quad V_\omega = \int \int |f'_\omega(v)| f(v) dv d\omega.$$

To see if this theorem is useful for natural coin-tosses, we carried out empirical measurements similar to those reported in Section 5 below. These show that natural coin-tosses (approximately one foot tosses of duration about 1/2 second) have initial conditions concentrated on

$$(*) \quad 36 \leq \omega \leq 40, \quad 7 \leq v_z \leq 9$$

with ω measured in rev/sec and v_x measured in ft/sec. Putting the uniform distribution on the square in (*), Engel's Theorem gives

$$\left| P\{\text{heads}\} - \frac{1}{2} \right| \leq .056.$$

All of the studies cited above assume the coin is caught in the hand without bouncing. An analysis of the effect of bouncing in coin-tossing was suggested by [Vulovic and Prange, 1986]. Following Keller, they assume that the coin rotates about an axis through its plane. Thus, the phase space is (w, t) as before. They hypothesize an explicit model for inelastic collisions that determines the coins eventual resting place. The resulting partitioning of (ω, t) space is surprisingly similar to Kellers (Figure 6 , above). The analysis above as displayed in Figure 6 shows a reasonably fine partitionning of the phase space. In these regions, Vulovic and Prange show that bouncing causes a fractal structure to appear in regions far from zero. Then bouncing appreciably enhances randomness. [Zeng-yuan and Bin, 1985] carry these considerations forward. They include both bouncing and air resistance. In their model, bouncing, a very non-linear phenomena causes very pronounced sensitivity to initial conditions. They neglect precession and so do not encounter our phenomenon of unfair coins in the limit as (ω_N, t) increase.

An intriguing analysis of coin-tossing appears in [Jaynes,1996] Section 10.3. As a physicist, Jaynes clearly understands that conservation of angular momentum is the key to the analysis of coin-tossing. With hindsight, we can find our statement following Theorem 1 of Section 1, that if the angle ψ is sufficiently acute, then the coin remains same side up

throughout its trajectory. This result was also described to us by Alar Toomre in a 1981 personal communication. Jaynes discusses weighted coins and coins spun on the edge. He includes some data, in which a jar lid is tossed or spun in various ways and extreme biases ensue.

We turn next to a different method of randomizing: coins spun on their edge. Here, the situation is much changed. Spun coins can exhibit huge biases. The exact determination of the bias depends in a delicate way on the shape of the coin's edge and the exact center of gravity. Indeed, magicians use coins with slightly shaved edges, invisible to the naked eye, which always come up heads. While we will not pursue the details, we offer Figure 7 as evidence. This shows data provided by Jim Pitman from a class of 103 Berkeley undergraduates who were asked to (a) toss a penny 100 times and record head or tail, (b) spin the same penny 100 times and record head or tail. A histogram of the data appears in Figure 7. The tossed coins are absolutely typical of fair coins, concentrated near 50 heads. The spun coins show pronounced bias towards tails; several students had coins that came up fewer than 10% heads. For further discussion, see [Snell et al, 2002].

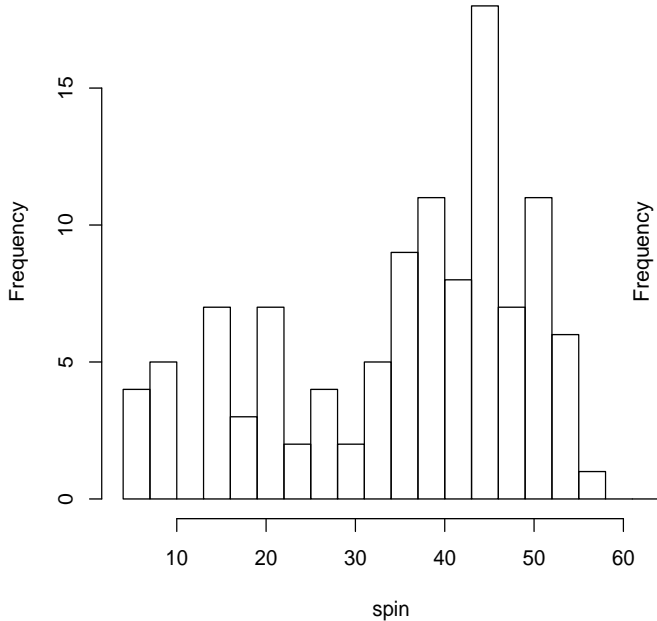


Figure 7a: Coins spun on their edges

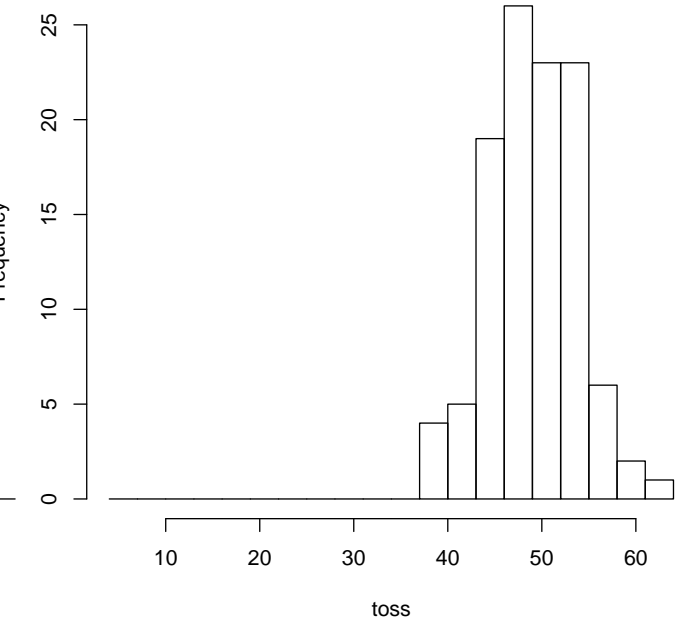


Figure 7b: Tossed Coins

If a coin is flipped up and allowed to bounce on the floor, our observations suggest that some of the times it spins around a bit on its edge before coming to rest. If this is so, some of the strong edge spinning bias comes into play. There may be a real sense in which tossed coins landing on the floor are less fair than when caught in the hand. People often feel the other way. But we suggest that this is because coins caught in the hand are easier to

manipulate. While this is clearly true, ruling out dishonesty, we stick to our conjecture.

Throughout, we have neglected the possibility of coins landing on their edge. We make three remarks in this direction. First, as a youngster, the first author was involved in settling a proposition bet where 10 coins were tossed in the air to land on the table (this to be repeated 1000 times). On one of the trials, one of the coins spun about and landed on its edge. [Murray and Teare, 1993] have developed an analysis of coins landing on edge. Using a combination of theory and experiment they conclude that an American nickel will land on its edge about one in 6000 tosses. Finally, [Mosteller, 1987] develops tools to study the related question “how thick must a coin be to have probability 1/3 of landing on edge?”

In light of all the variations, it is natural to ask if inhomogeneity in the mass distribution of the coin can change the outcome. [Lindley, 1981] followed by [Gelman & Nolan, 2002] give informal arguments suggesting that inhomogeneity doesn’t matter for flipped coins caught in the hand. Jaynes reports that 100 flips of a jar lid showed no evidence of bias. We had coins made with lead on one side and balsa wood on the other. Again no bias showed up. All of this changes drastically if inhomogeneous coins are spun on the table (they tend to land heavy side up). As explained above, some of this bias persists for coins flipped onto a table or floor.

Coin-tossing is such a familiar image that it seems that someone, somewhere must have gathered empirical data. The only extensive data we have found is [Kerrich, 1946]’s heroic collection of 10,000 coin flips. Kerrich’s flips allowed the coin to bounce on the table so our analysis doesn’t apply. His data does seem random ($p = 1/2$) for all practical purposes. Our estimate of the bias for flipped coins is $p \doteq .51$. To estimate p near 1/2 with standard error 1/1000 requires $\frac{1}{2\sqrt{n}} = 1/1000$ or $n \doteq 250,000$ trials. While not beyond practical reach, especially if a national coin-toss was arranged, this makes it less surprising that the present research has not been empirically tested.

3. Rigid Body Motion

This section sets up notation, reviews needed mechanics and proves extensions of Theorems 1 and 2. Before plunging into details, it may be useful to have the following geometric picture of a tumbling, flipping coin. Suppose the coin starts heads up with the normal \vec{N} to the coin pointing upward in direction \vec{K} . The initial velocities determine a fixed vector \vec{M} (the angular momentum vector). Picture this riding along with the coin, centered at the coin’s center of gravity, staying in a fixed orientation with respect to the coordinates of the room. The normal to the coin stays at a fixed angle ψ to \vec{M} and rotates around \vec{M} at a fixed rate ω_N . At the same time, the coin spins (or precesses) in its plane about \vec{N} at a fixed rate ω_{pr} . This description is carefully derived in Section 3.1. Theorem 1 is proved in Section 3.2 allowing the initial configuration of the coin to be in general position. The amount ΔA of

precession during one revolution of \vec{N} about \vec{M} is related to the angle ψ by $\Delta A \doteq \pi \cos(\psi)$. This is made precise in two ways in Section 3.3 where it is seen as a kind of ‘Berry phase’. As described there, we found this a convenient way to empirically estimate the crucial angle ψ .

This section uses the notation and development of [Landau & Lifschitz, 1976], Chapter 6. A more introductory account of the mysteries of angular momentum appears in [Feynman et al., 1963], vol I, chapters 18-20. The classical account of [Goldstein, 1950] spells out many details. An advanced treatment appears in [Marsden & Ratiu, 1994].

3.1 The Basic Setup

We model the flipping coin as a homogeneous, symmetric rigid body. Its center of gravity \vec{R}_G moves according to $\vec{R}_G(t) = (X(0) + tV_x, Y(0) + tV_y, Z(0) + tV_z - gt^2/2)$ where $\vec{V} = (V_x, V_y, V_z)^T$ is its initial velocity, and where the last coordinate is direction of gravity. In order to describe the tumbling of the coin we use two coordinate systems, both centered at \vec{R}_G . One has its axes directions fixed relative to an inertial, or laboratory frame. Coordinates and vectors in this system are denoted by capital letters. The second coordinate system has its axes rigidly attached to the coin, and is called the body frame, and its coordinates and vectors are denoted by small letters. For example, the normal to the coin as viewed from the laboratory frame is \vec{N} and depends on time, while the same normal, viewed in the body frame is written \vec{n} and is a constant vector along the z axis. The two frames are related by a rotation matrix $\Gamma(t)$ which takes a vector in the body frame, to the same point in the laboratory frame. Thus, for example $\vec{N}(t) = \Gamma(t)\vec{n}$. For more on moving frames, such as the body frame, see for example [Flanders, 1963] for an introductory account.

The instantaneous angular velocity $\vec{\Omega}(t)$ is a way of encoding the time-derivative of $\Gamma(t)$. It is a vector such that if \vec{X} is pointing to a fixed material point on the coin, so that $\vec{X}(t) = \Gamma(t)\vec{x}$ with \vec{x} constant in the body frame, then

$$(3.1) \quad \frac{d\vec{X}}{dt} = \vec{\Omega}(t) \times \vec{X}.$$

It will be important to have a picture of the general solution to (3.1) in the case where $\vec{\Omega}(t) = \vec{\Omega}$ is constant. Then the projection of $\vec{X}(t)$ onto the line through $\vec{\Omega}$ is constant, while the projection of $\vec{X}(t)$ onto the perpendicular plane to $\vec{\Omega}$ traverses a circle at constant angular speed $\|\vec{\Omega}\|$. Putting these two motions together, $\vec{X}(t)$ sweeps out a cone, whose tip travels the circle centered at the projection of $\vec{X}(0)$ onto the line through $\vec{\Omega}$, with the plane of this circle perpendicular to this line.

In general, $\vec{\Omega}(t)$ changes with t . There are exactly two cases where $\vec{\Omega}(t)$ is constant: the total cheat coin, and the Keller coin as discussed in section 1. Suppose that the coin

starts heads up with the normal pointed up (in direction \vec{K}). For the ‘total cheat coin’, $\vec{\Omega}(t)$ is vertical, in line with the normal to the coin, and its length is constant. Then, the coin remains horizontal for all time and spins about the normal direction with some constant angular speed ω (the length of $\vec{\Omega}(t)$). Equation (3.1) becomes

$$\frac{d\vec{X}}{dt} = \omega \vec{K} \times \vec{X}.$$

For the ‘fair coin’ analyzed by Keller, $\vec{\Omega}(t)$ lies in the plane of the coin. If its direction is along \vec{I} then (3.1) become $\frac{d\vec{X}}{dt} = \omega \vec{I} \times \vec{X}$ where again ω is the length of the (constant) vector $\vec{\Omega}(t)$. This story was told in Section 2. In all other cases, $\vec{\Omega}(t)$ depends on t .

The evolution of the angular velocity can be determined by using the conservation of angular momentum and the linear relation between angular momentum and angular velocity. While we will not need it explicitly, the angular momentum vector \vec{M} for a rigid body may be defined as a sum over particles in the body:

$$(3.2) \quad \vec{M} \doteq \sum_a m_a \vec{R}_a \times \vec{V}_a$$

with \vec{R}_a the position of the a^{th} particle from the center of gravity, \vec{V}_a its velocity, and m_a its mass. Conservation of angular momentum asserts that \vec{M} is constant during the flight of the coin.

The vectors \vec{M} and $\vec{\Omega}(t)$ are related by a symmetric positive definite matrix called the moment of inertia tensor ([Landau & Lifschitz, 1976], Sec.32). This matrix is constant relative to the body frame. Its eigenvalues are called the principle moments of inertia and denoted I_1, I_2, I_3 . Because of the coin’s symmetry, $I_1 = I_2$ and the eigenvectors for I_1, I_2 span the plane of the coin. Call them \vec{e}_1, \vec{e}_2 . The eigenvector for I_3 is \vec{n} , the normal to the coin. If the coin is modeled as a solid cylinder of thickness h , radius ρ , and uniform density, then [Landau & Lifschitz, 1976], pg. 102 2(c) shows that

$$(3.3) \quad I_1 = I_2 = \frac{1}{4}m\rho^2 + \frac{1}{3}mh^2 \quad \text{and} \quad I_3 = \frac{1}{2}m\rho^2$$

where m is the total mass. Note that in the $h \downarrow 0$ limit (a very thin coin) $I_1 \sim I_3/2$. The experiments described in Section 5 use an American half dollar which has

$$h = 2.15\text{mm}, \rho = 15.3\text{mm}, m = 11.34\text{g} \quad \text{thus} \quad I_1 = I_2 = 0.681\text{g.m}^2 \quad \text{and} \quad I_3 = 1.327\text{g.m}^2$$

Let $\vec{\omega}$, \vec{m} be the angular velocity and angular momentum in the body frame. Thus $\vec{\omega} = \Gamma(t)^{-1}\vec{\Omega}$ and $\vec{m} = \Gamma(t)^{-1}\vec{M}$. Expanding them out in terms of the eigenframe $\vec{e}_1, \vec{e}_2, \vec{n}$ yields

$$\vec{\omega} = \omega_1 \vec{e}_1 + \omega_2 \vec{e}_2 + \omega_3 \vec{n}$$

$$\vec{m} = m_1 \vec{e}_1 + m_2 \vec{e}_2 + m_3 \vec{n}$$

The components ω_i and m_i will depend on t in general. Applying the moment of inertia tensor to $\vec{\omega}$ yields \vec{m} :

$$(3.4) \quad \begin{aligned} \vec{m} &= I_1 \omega_1 \vec{e}_1 + I_2 \omega_2 \vec{e}_2 + I_3 \omega_3 \vec{n} \\ &= I_1 \vec{\omega} + (I_3 - I_1) \omega_3 \vec{n} \end{aligned}$$

where we have used that $I_1 = I_2$. We now apply the rotation matrix $\Gamma(t)$ relating the two frames to obtain:

$$\vec{M} = I_1 \vec{\Omega} + (I_3 - I_1) \omega_3 \vec{N}$$

Solving for $\vec{\Omega}$ gives

$$(3.5) \quad \begin{aligned} \vec{\Omega} &= \frac{1}{I_1} \vec{M} + \left(1 - \frac{I_3}{I_1}\right) \omega_3 \vec{N} \\ &= \omega_N \widehat{\vec{M}} - \omega_{pr} \vec{N} \end{aligned}$$

where

$$(3.6) \quad \omega_N = M/I_1, \omega_{pr} = \left(\frac{1}{I_1} - \frac{1}{I_3}\right) M \cos(\psi), \quad \widehat{\vec{M}} = \vec{M}/M$$

and $M = \|\vec{M}\|$ is the magnitude of the angular momentum \vec{M} , and where we have used $M_3 = M \cos(\psi) = I_3 \omega_3$. We note that ω_{pr} is positive since $I_1 < I_3$.

The vectors \vec{M} and $\vec{\Omega}(t)$ are parallel precisely at the extremes of the total cheat coin and the fair coin. In the total cheat case the components $\omega_1 = \omega_2 = 0$, the vectors \vec{M} and \vec{N} are proportional and constant in time, and $\vec{M} = I_3 \vec{\Omega}$, so that $\vec{\Omega}$ is also constant in time. In the fair case the component ω_3 is zero and $\vec{M} = I_1 \vec{\Omega}$ and again $\vec{\Omega}$ is constant in time. In all other cases; the angular momentum and velocity vectors are not parallel. The vector \vec{M} stays constant in laboratory coordinates while \vec{N} and $\vec{\Omega}$ move in laboratory coordinates.

From (3.1) and (3.4)-(3.6) we can read off the geometric description which introduced this section. Equation (3.1) applies to the vector $\vec{X} = \vec{N}$ since \vec{n} is fixed in the coin frame. Thus

$$\frac{d\vec{N}}{dt} = \vec{\Omega}(t) \times \vec{N}.$$

Then, (3.5) along with $\vec{N} \times \vec{N} = 0$ imply

$$(3.7) \quad \frac{d\vec{N}}{dt} = \omega_N \widehat{\vec{M}} \times \vec{N}.$$

This equation asserts that the coin's normal vector precesses about the axis \widehat{M} and that the angular frequency of precession is $\omega_N = M/I_1$, as in (3.6). The following section solves (3.7) and uses this to prove proposition 1.

3.2 A Generalization of Theorem 1

In the inertial frame \vec{K} is the up direction, \widehat{M} is the unit vector in the direction of the angular momentum and $\vec{N}(t)$ is the unit normal to the head of the coin. The coin is 'up' if $\vec{K} \cdot \vec{N} > 0$ and 'down' (tails) if $\vec{K} \cdot \vec{N} < 0$. Theorem 1 assumes that the coin starts with heads perfectly up ($\vec{K} = \vec{N}$ at time 0). The following extensions allow an arbitrary start for \vec{N} .

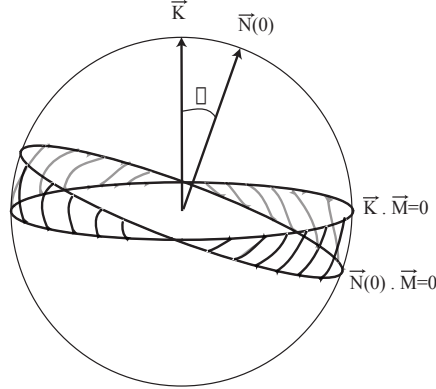


Figure 8: The situation of Theorem 1*. $\vec{N}(0)$ and the vertical \vec{K} need not be equal.
When \widehat{M} is in the shaded region the asymptotic bias is towards tails.

Theorem 1* Let $f(t) = \vec{N}(t) \cdot \vec{K}$ be the quantity which determines 'Heads' or 'Tails', i.e the cosine of the angle between the normal $\vec{N}(t)$ to the coin at time t and the up direction \vec{K} . Define ψ, ϕ by

$$\cos(\psi) = \vec{N}(0) \cdot \widehat{M}$$

$$\cos(\phi) = \vec{K} \cdot \widehat{M}$$

then

$$f(t) = A + B \cos(\omega_N t + \theta_0)$$

with $A = \cos \psi \cos \phi, B = \sin \psi \sin \phi, \omega_N = M/I_1$ for I_1 given by (3.3), and the phase θ_0 is determined by $\vec{K} \cdot \vec{N}(0)$.

Note that when $\vec{N}(0) = \vec{K}$ so the coin starts heads 'exactly' up, then $\psi = \phi$ and Theorem 2 yields Theorem 1. (We will see in the proof –look at the definition of \widehat{G}_1 there – that in this case $\theta_0 = 0$ also.)

We have presented figure 8 in order to help interpret Theorem 1* and Theorem 2*. Figure 8 represents a sphere of possible unit vectors \widehat{M} , with the two points $\vec{N}(0)$ and \vec{K} indicated, along with their corresponding great circles (“polars”) which are the locus of points where $\vec{N}(0) \cdot \widehat{M} = 0$ and where $\vec{K} \cdot \widehat{M} = 0$. The shaded region between these great circles is the region where \widehat{M} must be located in order for the coefficient A to be negative, and consequently in this region (see Theorem 2*) the asymptotic bias is towards tails as opposed to heads.

Proof From (3.7) for any $t \geq 0$, $\cos \psi = \vec{N}(0) \cdot \widehat{M} = \vec{N}(t) \cdot \widehat{M}$: the normal to the coin makes a constant angle with the angular momentum vector. Introduce a new orthonormal basis for space $(\widehat{G}_1, \widehat{G}_2, \widehat{M})$, with \widehat{G}_1 in the plane spanned by \widehat{M} and \vec{K} , so that \widehat{G}_2 is perpendicular to both \widehat{M} and \vec{K} . Then, from the definition of ϕ

$$\vec{K} = \sin(\phi)\widehat{G}_1 + \cos(\phi)\widehat{M}.$$

The general solution of the first order linear differential equation (3.7) for $\vec{N}(t)$ is $\vec{N}(t) = a\widehat{M} + b(\widehat{G}_1 \cos(\omega_N t + \theta_0) + \widehat{G}_2 \sin(\omega_N t + \theta_0))$. The initial value of $\vec{N}(0) \cdot \widehat{M}$ determine $a = \cos(\psi), b = \sin(\psi)$. (The value of θ_0 can be determined from $\vec{N}(0) \cdot \vec{K}$ if needed.) Altogether

$$\vec{N}(t) = \cos(\psi)\widehat{M} + \sin(\psi)\{\cos(\omega_N t + \theta_0)\widehat{G}_1 + \sin(\omega_N t + \theta_0)\widehat{G}_2\}.$$

The expression for $f(t) = \vec{N}(t) \cdot \vec{K}$ follows from the orthonormality of $(\widehat{G}_1, \widehat{G}_2, \widehat{M})$. This completes the proof of Theorem 1 as well. ■

The analytic argument of the next section shows that for vigorously flipped coins the argument $\omega_N t$ of f in Theorem 1* is asymptotically uniformly distributed (mod 2π). The following Theorem extends Theorem 2 to the case where the coin doesn’t start with head perfectly up.

Theorem 2* Let $\psi, \phi, 0 \leq \psi, \phi \leq \pi/2$ be defined as in Theorem 1*. Let $p(\psi, \phi)$ be the limiting probability of heads for a coin leaving the head with angle ψ between the normal $\vec{N}(0)$ to the coin and angular momentum \vec{M} and angle ϕ between the up direction \vec{K} and \vec{M} . Then

$$p(\psi, \phi) = \begin{cases} \frac{1}{2} + \frac{1}{\pi} \sin^{-1}(\cot(\phi) \cot(\psi)) & \text{if } (\cot \phi)(\cot \psi) \leq 1 \\ 1 & \text{if } (\cot(\phi)) \cot(\psi) \geq 1. \end{cases}$$

Proof According to Theorem 4 of the next section, the angle $\theta = \omega_N t$ is uniformly distributed on $[0, 2\pi)$ in the limit. We must then evaluate the probability that $f(\theta) > 0$ where, with θ uniformly distributed and f is the function of Theorem 1*. We have $f(\theta) = A + B \cos(\theta)$ with $A = \cos(\psi) \cos(\phi)$, $B = \sin(\psi) \sin(\phi)$. If $A > B$ then $f(\theta) > 0$ for all θ and $p = 1$. This

happens if and only if $\cot(\phi) \cdot \cot(\psi) > 1$. To compute in the case $A \leq B$ observe that f is symmetric about $\theta = \pi$ and is monotone decreasing on $(0, \pi)$. It follows that f has a unique zero θ_1 in $(0, \pi)$, that f is positive on $0 < \theta < \theta_1$, and that f is negative on $\theta_1 < \theta \leq \pi$. The uniform measure of the set $\{\theta : f(\theta) > 0\}$ is then

$$p(\psi, \phi) = \theta_1/\pi.$$

The zero θ_1 occurs when $\cos(\theta) = -A/B$. So $\theta_1 = \cos^{-1}(-A/B)$.

Using $\cos\left(\frac{\pi}{2} + h\right) = -\sin(h)$ gives $\theta_1 = \frac{\pi}{2} + \sin^{-1}(A/B)$. Finally, $A/B = \cot \phi \cot \psi$. ■

This completes the proof of Theorem 2 as well.

3.3 Precession of the Head

As explained in the introduction to this section, while the normal to the coin is spinning about the angular momentum vector at rate ω_N , the coin is also spinning about the normal at a constant rate ω_{pr} . We now further quantify and verify that assertion. For background on *Berry phase* see [Montgomery, 1991].

Theorem 3. With notation as in (3.3), (3.6), each time the normal vector completes one full cycle around the angular momentum vector, the coin has precessed by the angle:

$$(3.8a) \quad \Delta A = -\frac{\omega_{pr}}{\omega_N} 2\pi = -(1 - I_1/I_3) 2\pi \cos(\psi)$$

$$(3.8b) \quad \sim -\pi \cos(\psi) \quad \text{as } h \downarrow 0.$$

Remark: When $\psi \simeq 0$ so that \vec{M} is nearly aligned with the vertical, we have $\Delta A \simeq \pi$. In other words, every time the normal vector precesses around once, the coin rotates approximately 180° . Feynman observed this phenomenon in a Cornell dining hall. In his own words:

“some guy, fooling around, throws a plate in the air”. By noticing the difference between the plate’s angular velocity and that of the associated wobble, says Feynman, he was motivated to higher things: “The diagrams and the whole business that I got the Nobel Prize for came from that piddling around with the wobbling plate” [Feynman & Leighton, 1985]

Remark. While the angular momentum and ψ are difficult to measure directly, the slow motion photography explained in Section 5 often produced two frames where the coin clearly completed one revolution and the angle ΔA can be measured. From (3.8b), this gives ψ . An example is shown in Figure 9. We have two methods for estimating ψ from photographs:

using this ‘Berry phase’ from Theorem 3, or reconstructing the normal’s time evolution and figuring out the radius of the resulting circle on the sphere. We have used four such tosses to check the two methods, for instance for toss No 27, we have an estimate of $\hat{\psi} = 1.48$ with the Berry phase method and for Tosses No 30: $\hat{\psi} = 1.47$ and for Toss No 32: $\hat{\psi} = 1.40$, and for Toss No 33: $\hat{\psi} = 1.36$.

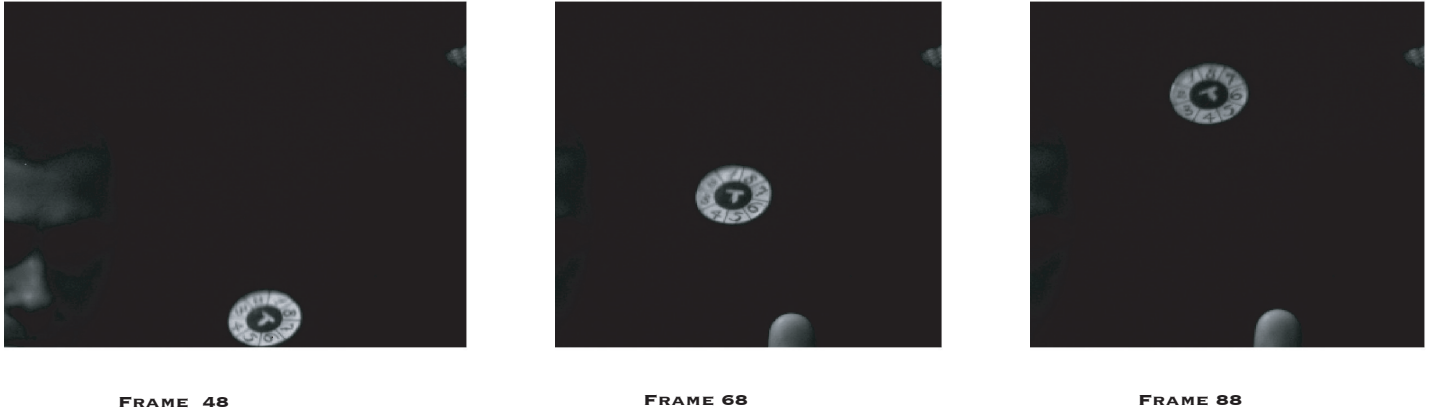


Figure 9: Berry Phase, these images are separated by exactly one coin flip.

Proof: Our proof relies on Euler’s description of the motion of a rigid body, essentially the dual to equation (3.1) ([Landau & Lifschitz, 1976], sec.36,36.5-36.7). Let \vec{X} be a vector which is fixed in space, and let \vec{x} be the corresponding vector, viewed in the body frame. Then Euler asserts that $d\vec{x}/dt = -\omega(t) \times \vec{x}$. Euler’s equation is obtained by taking for \vec{X} the angular momentum \vec{M} :

$$d\vec{m}/dt = -\omega(t) \times \vec{m}$$

Since $\omega = \omega_N \vec{m} - \omega_{pr} \vec{n}$ (see eq. (3.5)) and since $\vec{m} \times \vec{m} = 0$ Euler’s equation becomes:

$$(3.9) \quad d\vec{m}/dt = \omega_{pr} \vec{n} \times \vec{m}$$

To complete the proof, we have $\vec{N}(T) = \vec{N}(0)$ where $T = 2\pi/\omega_N$ is the period of \vec{N} ’s precession. The evolution equation (3.9) for \vec{m} asserts that the projection \vec{b} of \vec{m} onto the plane of the coin precesses at frequency ω_{pr} relative to a frame rigidly attached to the coin. (See the geometric description following eq. (3.1).) Consequently, after time T the vector \vec{b} has rotated by an amount $\omega_{pr}T$. In the meantime, in the lab frame the plane of the coin has returned to its original position and the vector \vec{M} has not moved. But \vec{b} is simply the projection of \vec{M} , viewed relative to the coin’s frame. It follows that the coin’s frame has rotated by $-\omega_{pr}T = \Delta A$ about the normal in the same time. ■

4. Uniformity of Angular Distribution.

The proof of Theorems 2, and 2* rely on the assertion that $\theta = \omega_N t$, modulo 2π , tends to the uniform distribution on the interval $[0, 2\pi)$. It remains to establish this uniformity. The key is a theorem stating that if we take any ‘nice’ real random variable X , rescale it, and view the result modulo 2π , then as the rescaling tends to infinity, the distribution of the random variable becomes uniform. In symbols: $\lambda X \bmod 2\pi$ tends to the uniform distribution U on the interval $[0, 2\pi)$ as $\lambda \rightarrow \infty$. This scaling theorem is to be found in the book by Engel discussed further below.

The product $\omega_N t (\bmod 2\pi)$ depends on the initial conditions:

$$\omega_N = \|\vec{M}\|/I_1 \quad \text{and} \quad t = t_c = v_z/(g/2)$$

(See (3.3) and (3.6).) For vigorously flipped coins $\|\vec{M}\|$ and v_z will be large. To formalize this “largeness” we suppose that the joint probability distribution of $\omega = \omega_N$ and t is of the form $g(\omega - \omega_0, t - t_0)$ where ω_0 and t_0 are large, and where $g(\omega, t)$ is a smooth probability density (C^1 is enough) with compact support. Note in particular that the expectation of ω is of order ω_0 , and of t is of order t_0 .

The argument we are about to present is a variant of one due to E. Engel and J. Kemperman, and developed in Chapters 2, 3, of [Engel, 1992]. This book is strongly recommended.

For ease of notation and proof we abstract. Let (X_λ, Y_λ) be a family of real valued random variables parameterized by the ray $0 < \lambda < \infty$. The following two assumptions are needed

(4.1) For some $c > 0$ there is a $\gamma > 0$ so that for all λ

$$P\{Y_\lambda < \lambda c\} \leq \gamma/\lambda$$

(4.2) For each λ and each fixed y , there is a regular conditional probability distribution for X_λ given $Y_\lambda = y$, with differentiable density $p_{X_\lambda}(x|Y_\lambda = y)$ satisfying

$$\int |p'_{X_\lambda}(x|Y_\lambda = y)| p_{Y_\lambda}(dy) = A_\lambda < \infty.$$

Assumption 4.1 is a way of saying that $Y_\lambda \rightarrow \infty$ with λ . Assumption 4.2 is a way of saying that the marginal density X_λ at x , which is $\int p_{X_\lambda}(x|Y_\lambda = y) p_{Y_\lambda}(dy)$, is not too sharply peaked for any x .

In our application λ parametrizes a ray in the positive ω, t orthant, $X_\lambda = \omega_N$, $Y_\lambda = t_c$ are distributed according to $g(\omega - \lambda\omega_0, t - \lambda t_0)$. For g smooth with compact support, both conditions (4.1) and (4.2) are satisfied with A_λ uniformly bounded.

The statement of the next theorem involves the variation distance between two measures μ, ν . This is defined by

$$\begin{aligned} d_v(\mu, v) &= \sup_C |\mu(C) - v(C)| \\ &= \frac{1}{2} \int \left| \frac{d\mu}{d\sigma} - \frac{dv}{d\sigma} \right| d\sigma \end{aligned}$$

with the sup over all measurable sets C . In the second equality σ is any measure which dominates both μ and v (for example $\sigma = \mu + v$). Note that this second equality is independent of σ . If X and Y are random variables with $\mu(C) = P(X \in C)$, $\nu(C) = P(Y \in C)$ we write $d_v(X, Y)$ for $d_v(\mu, \nu)$. A careful treatment of variation distance is [Engel, 1992].

Theorem 4 Let (X_λ, Y_λ) be a family of real valued random variables satisfying (4.1), (4.2). Let U be a uniform random variable taking values on the interval $[0, 2\pi]$. Then, for all λ

$$d_v(X_\lambda Y_\lambda \text{mod}2\pi, U) \leq \frac{\gamma}{\lambda} + \frac{\pi}{4c} \frac{A_\lambda}{\lambda}.$$

Proof

$$\begin{aligned} d_v(X_\lambda Y_\lambda \text{mod}2\pi, U) &\leq \int d_v(X_\lambda y \text{mod}2\pi, U) P_{y_\lambda}(dy) \\ &\leq P\{Y_\lambda \leq c\lambda\} + \int_{\{Y_\lambda \geq c\lambda\}} d_v(X_\lambda y \text{mod}2\pi, U) P_{Y_\lambda}(dy) \\ &\leq \frac{\gamma}{\lambda} + \int_{\{Y_\lambda \geq c\lambda\}} \frac{\pi}{4y} \int |p'_{X_\lambda}(x|Y_\lambda = y)| dx P_{Y_\lambda}(dy) \\ &\leq \frac{\gamma}{\lambda} + \frac{\pi}{4c\lambda} A_\lambda. \end{aligned}$$

The first inequality follows from proposition 2.8a of [Engel, 1992]. This says that if X and Y are real valued random variables and Z is a random variable defined on the same probability space then

$$d_v(X, Y) \leq \int d_v(X^z, Y) P_z(dz)$$

with X^z the random variable conditional on $Z = z$. The second inequality uses $d_v \leq 1$. The third inequality uses (4.1) and Theorem 3.3 of Engel, the theorem mentioned in the first paragraph of the present section. This theorem states that for a real random variable X with differentiable density $p(x)$,

$$d_v(tX \text{mod}2\pi, U) \leq \frac{\pi}{4t} \int |p'(x)| dx.$$

the last equality uses Assumption (4.2). ■

Remarks

- 1) The roles of X_λ, Y_λ can be reversed and the minimum of the two resulting bounds used.

- 2) The rate of convergence, order $1/\lambda$, may be shown to be best possible. However, there are also classes of examples where the convergence in Theorem 3 is exponential in λ or even faster. See [Engel, 1992], Chapter 3 for the full range of possibilities.
- 3) In the present application, convergence of $X_\lambda Y_\lambda(\text{mod}2\pi)$ to U is used in conjunction with the $f(\theta)$ of Theorem 1* to obtain Theorem 2. Since the f is a bounded continuous function, weak-star convergence to U will do. [Engel, 1992] shows that $\lambda X(\text{mod}2\pi)$ weak-star converges to U if and only if the Fourier coefficients of $X(\text{mod}2\pi)$ converge to zero. Thus densities such as $g(\omega, t)$ are not required for Theorem 2 to hold.

5. Estimating Angular Momentum

The empirical distribution of the angle ψ between the angular momentum vector \vec{M} and the normal to the coin figures crucially in our analysis of coin tossing. In this section we describe our efforts at estimating this distribution for real flips of an American half dollar.

We carried out two types of experiments. Our “low-tech” experiment involved flipping a coin with a ribbon attached. After the flip the ribbon is unwound, showing how many times the coin rotated. This is carefully described in Section 5A. Our “high-tech” experiment involves a high speed camera and the mathematics of section three to estimate the sequence of normals to the coin at different times during the coin’s flight. These lie in a circle centered at the angular momentum vector. The radius of this circle gives an estimate of ψ . These results are described in Section 5.2. This estimate of ψ can be calibrated with the measured value of rotation of the coin’s face (the ‘Berry phase’) using the relation between this angle and ψ described in formula (3.8).

5.1 Coin and Ribbon A 1/8-inch wide 29-inch long ribbon was attached to an American half dollar with scotch-tape.

For each flip, the ribbon was flattened (untwisted), with the end held in the left hand. The coin was positioned heads up, in a fixed orientation in a fixed coordinate system marked on a table. The coin was given a normal flip with the right hand, caught without bouncing at approximately the same height. For all flips that resulted in heads up two numbers were recorded.

- The angle θ that a fixed point on the coin’s head made with its original starting orientation. Here $-180^\circ < \theta < 180^\circ$ with 180° and -180° indistinguishable. The angle was measured to the nearest 5° .
- The number f of complete flips of the coin, determined by unwinding the ribbon until it is untwisted.

Pairs (θ, f) were recorded for 100 flips. ($1 \leq i \leq 100$). A scatter-plot of these values appears in Figure 10. There are three noticeable features.

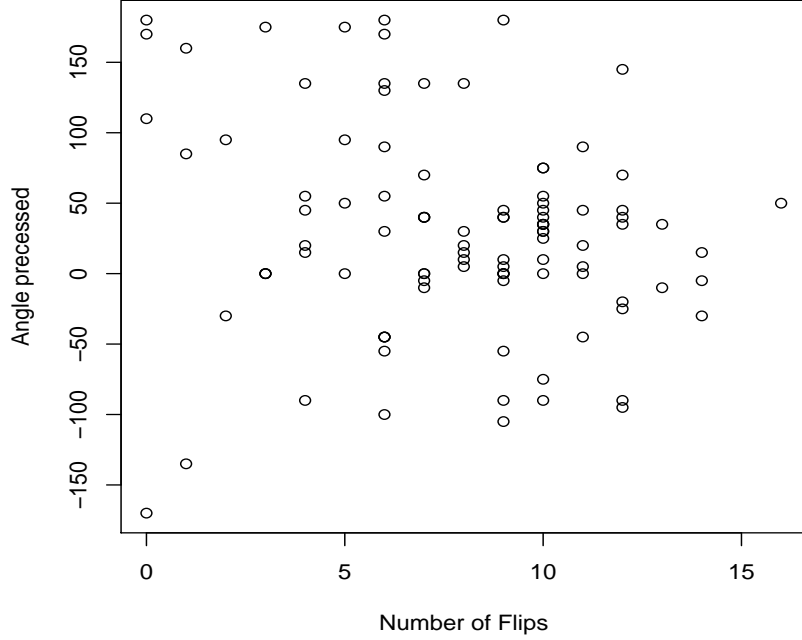


Figure 10: Scatterplot of ribbon data

1. Four of 100 flips have $f = 0$ (the coin never turned). These were vigorous flips with θ ranging widely. This indicates that the angular momentum vector make angle at most 45° with the normal roughly $1/25$. Re-enforcing this, three of 100 flips have $f \equiv 1$.
2. The angles θ vary widely. With a minimum of -170° ; lower quartile -1.3° , median and mean about 30° ; upper quartile of 55° and maximum of 180° . If the angular momentum vector was in the plane of the coin ($\psi = \pi/2$). All these θ_i would be zero.
3. The (θ, f) pairs seem independent of each other ($\text{corr} = -.2$). Indeed, the distribution of θ seems roughly uniform. One explanation is that the marked point on the coin makes several turns around.

All three observations re-enforce the idea that typical coin flips often have the angle ψ far from $\pi/2$.

5.2 Slow Motion Photography We used a high-speed slow motion camera to record fifty coin flips. The camera, developed by Stanford's digital photo program shoots at up to 1400 frames per second ([Ercan et al., 2002],[Kleinfelder et al., 2001]). We found it best to film at

about 600 frames per second. In contrast, the slow motion feature on standard camcorders shoot at about 60 frames per second. This is much too slow to give any useful data.

The data collection and processing led to interesting, difficult problems which we discuss in detail elsewhere. Briefly, our camera gave about 100 frames per flip. At 600 frames per second, this gives a window of 1/6 seconds to record. We found careful effort required to start the filming so that enough of the flip was recorded.

A successful filming results in up to 100 two-dimensional images. As explained below, a circular disc projected onto a plane results in an ellipse. We painted the coin with two colors, black outside and a white disk painted half way into the coin. These two overlapping circles enabled us to check the camera calibration using [Fremont & Chellali, 2002] and [Zhang, 1999]'s work.

To accurately fit the ellipse, we used Matlab's image analysis software to threshold each image and detect the edge of the coin. This provides a set of points approximately situated on the ellipse. Next, the least squares fit to the ellipse was determined using the approach of [Bookstein, 1979] adapted by [Gander et al. 1994]. These steps result in a fitted ellipse for each image (see Figure 12).

From each ellipse the major and minor axis were determined. From these, as described below, the normal to the coin in three dimensions can be estimated. As a check, we superimposed our fitted ellipses and normals on the sequence of images and viewed the resulting movie. The fits seemed consistently good although not perfect; particular difficulties are encountered when the coin is close to edge on. Then, the thickness of the coin's edge becomes an important factor. The sequence of (a) coin images (b) coins with fitted ellipses can be viewed by the reader at <http://www-stat.stanford.edu/~susan/coins/>

At this stage, for each flip, we have a sequence of fitted normal vectors in three dimensions, centered at the coin's center of gravity. According to the theory of Section 3, these normals lie on a circle centered at the fixed angular momentum vector. The radius of this circle thus gives an estimate of the angle ψ associated to the flip. Of course, the circles can be fit from just a few points. We used about 20 points/flip and again checked visually to see if these looked as if they lay on a circle. Some surprising results are described following the basic normal fitting algorithm which is described next.

The plane of the camera is fixed throughout. In spatial coordinates (X_1, X_2, X_3) , the $(X_1, X_2, 0)$ plane will be identified with the camera plane and the line $(0, 0, X_3)$ is the orthogonal to the camera plane. At a fixed time, the coin is in a fixed position in 3-space. The projection of a circle or disc onto a plane is an ellipse. We observe, and can accurately estimate, the major and minor axes of this ellipse. The assumption of orthographic projection implies that the length of the major axis is the same as the length of the diameter of

the coin. Without loss of generality we assume the coin has radius 1. Let $\vec{A} = (A_1, A_2, 0)$ be a unit vector in the plane of the camera centered at the ellipse center along the major axis. Let $\vec{B} = (B_1, B_2, 0)$ be an orthogonal vector along the minor axis. Thus $|\vec{A}| = 1$ and $|\vec{B}| = \cos \theta$ for some angle θ , $0 \leq \theta \leq \pi/2$. This description of \vec{A}, \vec{B} involves a choice of \pm sign which we will deal with in a moment.

Throughout, we assume that the coin has been parallel translated so that its center lines up with the center of the ellipse.

Let \vec{U}, \vec{V} be the unit vectors on the coin, which project to \vec{A}, \vec{B} respectively so that in fact $\vec{A} = \vec{U}$. Let $\vec{K} = (0, 0, 1)$ be the direction orthogonal to the camera plane.

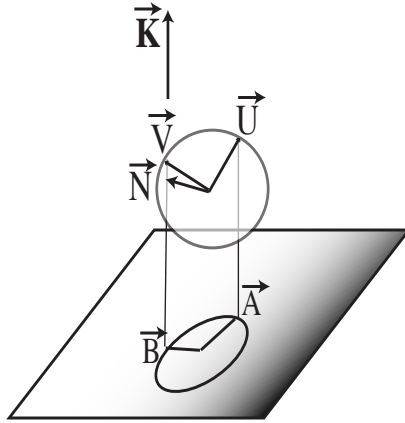


Figure 11: The disk shaped coin is projected onto an ellipse in the camera plane.

Lemma With notation as above the normal \vec{N} to the coin is

$$\vec{N} = (\epsilon_1 A_2 \sqrt{1 - (B_1^2 + B_2^2)}, \epsilon_2 A_1 \sqrt{1 - (B_1^2 + B_2^2)}, \epsilon_3 (A_1 B_2 - A_2 B_1))$$

for some choice of signs $\epsilon_i = \pm 1$.

Proof Any vector projecting onto \vec{B} has the form $\vec{V} = \vec{B} + \lambda \vec{K}$. Since our \vec{V} is a unit vector and $|\vec{B}| = \cos(\theta)$, $|\lambda| = \sin \theta$ is forced. Thus $\vec{N} = \vec{A} \times \vec{V} = \vec{A} \times (\vec{B} + \epsilon \sin \theta \vec{K})$. Expanding out the cross product and using $\sin \theta = \pm \sqrt{1 - (B_1^2 + B_2^2)}$ yields the result. ■

Remark The sign ambiguity creates a serious practical problem. If the coin is parallel to the plane of the camera, edge onto the camera the sign is difficult to determine. While these events happen rarely, with a tumbling coin, they do occur periodically and an arbitrary choice leads to physically ridiculous pictures. We resolve the choice of signs by continuity, choosing (at each time frame) the choice of eight sign patterns that makes the inner product

of the current normal and previous normal as close as possible to a constant, while keeping the curvature continuous.

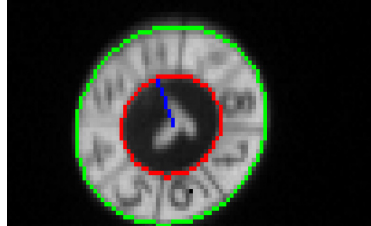


Figure 12: Fit of an ellipse to the image.

Figure 13b shows the result of this unscrambling process. In Figure 13a we see the sequence of 3-d normals as they come from the computation of normals one by one from the ellipses. There are some arcs (the successive normals are numbered in sequence), however the result is best described as a mess. In Figure 13b we see the unscrambled normals, unscrambled by appropriate choice of signs, all lie clearly around the circle. Our theory implies that these points lie in a plane in three dimensional space. We fit the plane using least squares. The distance between the plane and the origin gives us d from which we can find $\psi = \cos^{-1}(d)$.

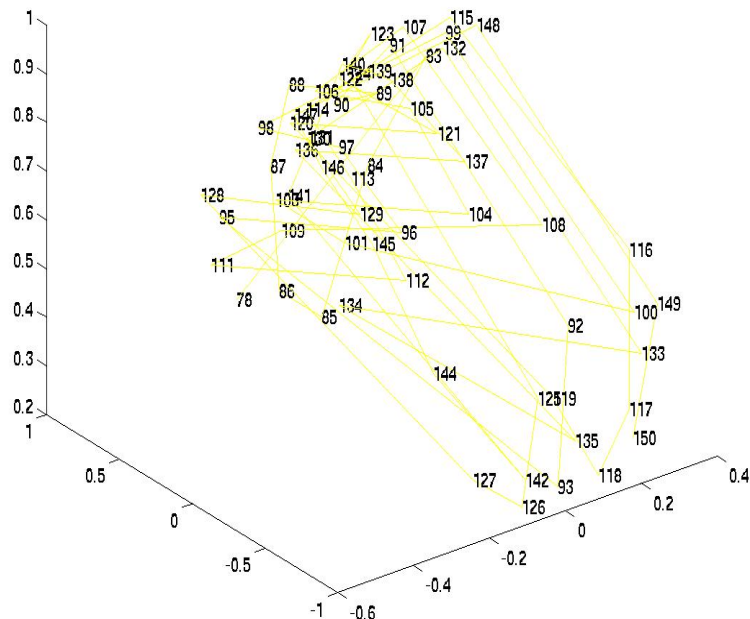


Figure 13a: The normals originally have a scrambled sign pattern.

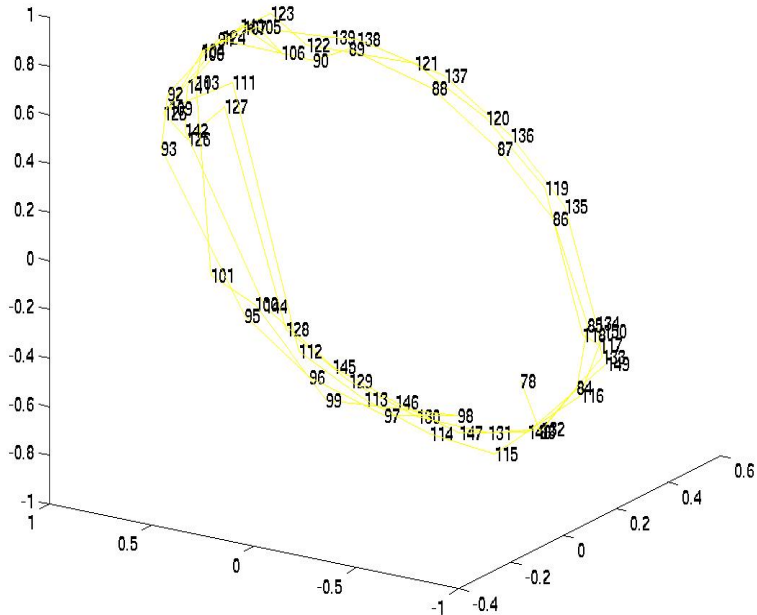


Figure 13b: How the normal vectors (once unscrambled) sit around a circle in 3-D.

The results: Of our 50 flips, 27 gave useful final results. From the measured values of ψ , the probability $p(\psi)$ was calculated from Theorem 2. The estimated probabilities range from 0.500 to 0.545. The 27 probabilities are displayed in a stem and leaf plot. The first row of this plot shows the values 0.500, 0.500, 0.501, ... indicating occurrences of flips for which $p(\psi)$ took on these values. The next-to-last row shows no occurrences between 0.540 and 0.545. The last row shows the single outlying value 0.545. Following this are the five number summary, the mean and the standard deviation.

50 | 0011111122233334

50 | 555

51 | 3

51 |

52 | 3

52 | 9

53 | 34

53 |

54 |

Five number summary of probabilities:

Min.	1st Qu.	Median	3rd Qu.	Max.
0.5001	0.5011	0.5027	0.5052	0.5448

Mean= 0.5083

sd = 0.0125

```
> psi
[1] 1.3697 1.2125 1.4682 1.2778 1.3103 1.2611 1.5528 1.4478 1.5211 1.5182
[11] 1.5100 1.2560 1.4797 1.4829 1.4705 1.5228 1.4696 1.5114 1.5102 1.4983
[21] 1.4962 1.4603 1.5176 1.4408 1.4519 1.5489 1.4800
> summary(psi)
  Min. 1st Qu. Median Mean 3rd Qu. Max.
1.213   1.444   1.480   1.446   1.511   1.553
> sd(psi)
[1] 0.09697983
> mean(psi)
[1] 1.446170
```

The mean of the probabilities is 0.508. We have rounded this up to the 0.51 quoted. For completeness the ψ values are also recorded, and we note that, if \bar{x} denotes the mean of x , $p(\bar{\psi}) \neq \overline{p(\psi)}$.

6. Some Caveats to the Analysis

In carrying through the present analysis we make a number of assumptions. In this section we point out naturally occurring situations where our assumptions are violated and hence our analysis need not apply.

6.1 Random In, Random Out We have assumed that the coin is flipped with a known side uppermost. In many occurrences of coin tossing a coin is removed from the pocket and hence may be assumed equally likely to start heads up as tails up. The physics preserves this: the outcome is equally likely to end heads up as tails up. We have friends who preface a coin toss by vigorously shaking the coin between their cupped hands.

6.2 No Air Resistance Throughout, we have neglected the effect of air resistance. Let us begin by acknowledging that air resistance is a potential confounding factor. Some friends in the physics department convinced us of this by dropping an American penny off Stanford's Hoover Tower. Some of the time it fell like a leaf, fluttering to the ground. We believe that for our short flips, air resistance has a negligible effect. One way to test this is to observe the

time t_1 that a coin takes to go from its start to the top of its trajectory and then the time t_2 that the coin takes to fall back to its initial starting height. As discussed in [Brauer, 2001] air friction forces $t_2 > t_1$. We expect the size of this effect to be very small and accurate measurement of it to be very difficult. [Zeng-yuan and Bin, 1985] include air resistance in their analysis of coin tossing, presuming the effect is proportional to velocity.

Careful modeling of a spinning coin in a retarding medium seems like a difficult problem. Even determining an appropriate approximation to the effect of friction on velocity is a contentious matter. Long and Weiss [Long & Weiss, 1999] discuss the classical assumption (frictional force proportional to velocity) in detail and argue that velocity raised to powers such as $3/2$ or 2 seems more appropriate.

6.3 Definition of Time in Flight We have used two different notions of the time t_c that the coin comes to rest (Section 3.1, 5.2). We have not incorporated the very real possibility that the time t_c has extra randomness due to the catcher's hand moving, or a psychological component due to the coin being caught early or late in its flight. We do not think that these variations in t_c materially affect our conclusions. The reason is that flipped coins (starting from heads up) simply spend more of their total time in flight heads up. Figure 4 shows this clearly. If the coin were caught at a completely random time (say uniformly chosen in a large interval) our analysis still applies.

6.4 Start Heads Up? Perhaps the most vulnerable assumption is the specification of the starting normal direction as heads exactly up. Careful observation of natural flips shows some play in the initial position due to the position of the hand and thumb. We have dealt with this mathematically in Section 3.2 but have not gathered data. Of course, this point is closely connected to 6.1 above.

6.5 No Bouncing We have assumed that the coin is caught without bouncing. While this is a very common occurrence, we note that often a flipped coin is caught in the hand and then slapped down on the table or on the back of the other hand, turning it over once. Of course, this last results in a bias opposite of the start. If the method of catching is not determined (sometimes flipped over, sometimes as fallen) a significant amount of randomness may be added.

Often, flipped coins are allowed to land on hard surfaces and bouncing occurs. This requires a different type of analysis. Some further discussion and references are in Section 2.

6.6 The pragmatic uncertainty principle. The measurements recorded in Section 5 may have affected the outcomes recorded. For example, attaching a ribbon to the coin changes the aerodynamics of its flight. To check this, we record the angle θ for 100 flips of a half dollar without the ribbon attached. The results were still widely spread out but now the

lower quantiles, median and upper quantiles were shifted to $-40^\circ, 0^\circ, 30^\circ$. Similarly; getting the slow motion camera in sync with our flips required fairly artful flips. These seem quite different from the more vigorous flips one observes at sporting events. We hope to develop a setup with multiple low speed cameras that allow measurement of more natural flips.

Conclusion: Despite these important caveats we find that the bias we have found fascinating. The discussion also highlights the true difficulty of carefully studying random phenomena. If we can find this much trouble analyzing a common coin toss, the reader can imagine the difficulty we have with interpreting typical stochastic assumptions in an econometric analysis.

The caveats and analysis also point to the following conclusion: For tossed coins, the classical assumptions of independence with probability 1/2 are pretty solid.

Acknowledgments:

Thanks to Ali Ercan, Abbas El Gamal for providing the camera images. Aharon Kapitulinik and Steve Shenker provided valuable advice about air resistance. Summer undergraduate student Varick Erickson, funded through a Stanford VPUE grant, refined the thresholding and edge detection procedures. Thanks to Vincent Fremont for his two circle calibration code. Jim Pitman for the Berkeley toss and spin data, M. Franklin for letting her technicians build the coin flipping machine. Joe Keller, for numerous conversations over the years. Jim Isenberg for an invitatioin to talk on an early version of this paper at the U. of Oregon. PD and SH acknowledge funding by NSF grant DMS 0101364 and RM by NSF grant DMS 0303100 .

References

- [Barnhart, 1992] R. Barnhart (1992) Beating the Wheel: Winning Strategies at Roulette, Lyle and Stuart, New York.
- [Bass, 1985] Bass, T. (1985) *The Eudaemonic Pie*, Houghton-Mifflin, Boston.

- [Bookstein, 1979] F. L. Bookstein, (1979) Fitting conic sections to scattered data, in Computer graphics & image processing 9, 56-71
- [Brauer, 2001] Brauer, F. (2001), What Goes Up Must Come Down, Eventually, *Amer. Math. Monthly* **108**, 437-440.
- [Doucet, 1998] Doucet, A. (1998) On Sequential Simulation-Based Methods for Bayesian Filtering, Technical report CUED/F-INFENG/TR.310, Cambridge Univ.
- [Engel, 1992] Engel, E. , (1992) *A Road to Randomness in Physical Systems*, Springer Verlag, NY.
- [Ercan et al., 2002] A. Ercan, F. Xiao, X.Q. Liu, S.H. Lim, A. El Gamal and B. Wandell, (2002), "Experimental High Speed CMOS Image Sensor System and Applications," Proceedings of IEEE Sensors Conference, pp. 15-20.
- [Fremont & Chellali, 2002] Fremont, V. and Chellali,R. (2002) Direct Camera Calibration using Two concentric Circles from a Single View. ICAT, pp. 93–98.
- [Faugeras, 1993] Faugeras,O. (1993) *Three-Dimensional Computer Vision*, MIT press.
- [Feynman et al.,1963] Feynman, R Leighton, R. and Sands,M (1963) *The Feynman Lectures on Physics*, vol I, Addison-Wesley, NY.
- [Feynman & Leighton, 1985] R. P. Feynman with R. Leighton (1985) *Surely You're Joking, Mr Feynman!* Norton, New York.
- [Gander et al. 1994] W.Gander, G.H. Golub, R. Strebel, (1994) Fitting of Circles and Ellipses : Least Square Solution, Tech report, SSCM, Stanford.
- [Flanders, 1963] Flanders, H. (1963). *Differential Forms with Applications to the Physical Sciences* (Dover reprint 1989 ed.). Mineola, N.Y.: Dover.
- [Gelman & Nolan, 2002] Gelman, A. and Nolan, D. (2002) You can load a die but you can't bias a coin, in Teaching Statistics. The American Statistician, pp 308-311.
- [Goldstein,1950] H. Goldstein, (1950) *Classical Mechanics*, Addison-Wesley, Reading, Mass.
- [Gordon et al., 1993] N.J. Gordon, D.J. Salmond and A.F.M. Smith, Novel Approach to Nonlinear/NonGaussian Bayesian State Estimation, IEE-Proceedings-F, vol. 140, no. 2, 1993, pp. 107-113.
- [Hopf,1934] Hopf, E. (1934) On Causality, Statistics and Probability, Journ Math. Physics, MIT, 13, 51-102.

- [Hopf,1936] Hopf, E. (1936) Über die Bedeutung der willkürlichen Funktionen für die Wahrscheinlichkeitstheorie. Jahresbericht Deutsche Math. Ver. 46, 179-195.
- [Hopf,1937] Hopf, E. (1937) Ein Verteilungsproblem bei dissipativen dynamischen Systemen, Mathematische Annalen, 114, 161-186.
- [Jaynes,1996] Jaynes, E. T. (1996). *Probability Theory: The Logic of Science*, pp. 1003–1007, Cambridge University Press, Cambridge.
- [Kanatani & Liu, 1993] K. Kanatani, and W. Liu, (1993), 3D Interpretation of Conics and Orthogonality, CVGIP : Image Understanding, vol. 58, No. 3, November, pp. 286-301.
- [Keller, 1986] J. B. Keller. (1986) The probability of heads, American Mathematical Monthly, 93:191-197.
- [Kerrich, 1946] Kerrich, J. E. (1946). *An Experimental Introduction to the Theory of Probability*, Copenhagen: J. Jorgensen.
- [Kim et al. , 2002] J. S. Kim, H. W. Kim, I. S. Kweon, (2002) A Camera Calibration Method using Concentric Circles for Vision Applications, ACCV2002, Melbourne, Australia.
- [Kleinfelder et al., 2001] S. Kleinfelder, S. Lim, X. Liu, and A. El Gamal (2001) A 10,000 Frames/s CMOS Digital Pixel Sensor, IEEE Journal of Solid State Circuits, Vol. 36, No. 12, pp. 2049-2059.
- [Landau & Lifschitz, 1976] Landau L. and Lifschitz, E, 1976, *Mechanics*, (3 ed), Pergamon Press, Oxford, UK.
- [Lindley, 1981] T. Foster Lindley (1981) Is it the coin that is biased? Philosophy, 56, p. 403–407.
- [Long & Weiss, 1999] Long, L and Weiss, H. (1999), The Velocity Dependence of Aerodynamic Drag: A Primer for Mathematicians, *Amer. Math. Monthly* **106**, 127-135]
- [Marsden & Ratiu, 1994] Marsden, J.E. and T.S. Ratiu (1994) *Introduction to Mechanics and Symmetry.*, Texts in Applied Mathematics, 17, Springer-Verlag, NY.
- [Montgomery, 1991] R. Montgomery (1991) How Much Does a Rigid Body Rotate?, Am. J. Physics,v. 59, no. 5, 394-398.
- [Mosteller, 1987] Mosteller, F. (1987) *Fifty Challenging Problems in Probability with Solutions*. New York: Dover.

- [Murray and Teare, 1993] Murray, D.B. and Teare, S.W. (1993) Probability of a tossed coin falling on its edge, Phys. Rev. E, 2547-2552.
- [Poincaré, 1896] Poincaré, H. (1896) *Calcul of Probabilités*, George Carré, Paris.
- [Snell et al, 2002] Snell, L., Peterson, B., Albert, J. and C. Grinstead (2002)
 Chance News 11.02, http://www.dartmouth.edu/~chance/chance_news/recent_news/chance_news_11.02.html
 Flipping, spinning and tilting coins
- [Strevens, 2003] Strevens, M. (2003) *Bigger than Chaos: Understanding Complexity through Probability*, Harvard University Press, Cambridge, MA.
- [von Plato, 1994] Von Plato, J. (1994) *Creating Modern Probability: Its Mathematics, Physics and Philosophy in Historical Perspective*, Cambridge University Press, Cambridge UK.
- [Vulovic and Prange, 1986] Vulovic, V. Z. and Prange, R. E. (1986) Randomness of a true coin toss. Physical Review A 33: 576-582.
- [Zhang, 1999] Zhang, Z. (1999), Flexible Camera Calibration by Viewing a Plane From Unknown Orientations, In Proc. 7 th International Conference on Computer, Greece, pp. 666-673.
- [Zeng-yuan and Bin, 1985] Yue Zeng-yuan and Zhang Bin, (1984), On the sensitive dynamical system and the transition from the apparently deterministic process to the completely random process, Applied Mathematics and Mechanics, vol.6, 3, 193–211.